

ARTICLE TYPE

Robust and accurate central algorithms for Multi-Component mixture equations with Stiffened gas EOS

Ramesh Kolluru^{1,4} | S V Raghurama Rao² | G N Sekhar³

¹Department of Aerospace Engineering,
Indian Institute of Science,
Bangalore, Karnataka, India

²Department of Aerospace Engineering,
Indian Institute of Science,
Bangalore, Karnataka, India

³Department of Mathematics, BMS College
of Engineering, Bangalore, Karnataka, India

⁴Department of Mechanical Engineering,
BMS College of Engineering,
Bangalore, Karnataka, India

Correspondence

*Ramesh Kolluru Email: kolluru@iisc.ac.in

Present Address

Post Doctoral Fellow, Department of
Aerospace Engineering, Indian Institute of
Science, Bangalore, Karnataka, India

Summary

Simple and robust algorithms are developed for compressible Euler equations with stiffened gas equation of state (EOS), representing gaseous mixtures in thermal equilibrium and without chemical reactions. These algorithms use fully conservative approach in finite volume frame work for approximating the governing equations. Also these algorithms used central schemes with controlled numerical diffusion for this purpose. Both Mass fraction (Y) and γ based models are used with RICCA and MOVERS+ algorithms to resolve the basic features of the flow fields. These numerical schemes are tested thoroughly for pressure oscillations and preservation of the positivity of mass fraction at least in the first order numerical methods. Several test cases in both 1D and 2D are presented to demonstrate the robustness and accuracy of the numerical schemes.

KEYWORDS:

MOVERS, MOVERS+, RICCA, Contact-discontinuity, γ - based approach

1 Introduction

Atmospheric air is a mixture of gases which are compressible in nature. Each of the components in the mixture have different physical and thermodynamical properties, and very often in modelling the flow, air is assumed to be a single component gas with constant properties. There are many applications where due consideration should be given to each of the components in the mixture such as gasoline and air mixture entering the combustion chamber and combustion products exhausting from the engines. There are instances where liquids and gases exist together like bubbles moving in the liquid, spray of paint facilitated through a nozzle. In all the situations mentioned above fluids exist as a mixture or as different components separated by interfaces.

Many times, the contribution of the individual components are negligible or the variation in the properties of the components do not contribute significantly to the flow field and hence they can be neglected. If the properties of the components vary at large, then the individual effect of the components are resolved or their combined effect on the mixture has to be studied. In these cases, the classic model of single component compressible fluid may not be appropriate.

Broadly the flow of these fluids can be classified into two categories: a) pure interface problems, and b) multicomponent flows. For pure interface problems, the thermodynamic properties of the fluids change only across the interface whereas in multicomponent flows the properties vary throughout the flow field. In pure interface problems, apart from solving for the dynamics of each component, the interface is also tracked by a specific method like level set method. In multicomponent flows the modelling is done without tracking any interface. Nature of multicomponent flows can vary from low subsonic flows to hypersonic reacting flows. Low subsonic flows often are coupled with combustion related phenomena and therefore are not easily amenable to numerical modelling. Modelling of supersonic and hypersonic flows can take advantage of the sophisticated numerical methods

⁰Abbreviations: MOVERS, Method of Optimum Viscosity for Enhanced Resolution of Shocks; RICCA Riemann Invariants based Contact-discontinuity Capturing Algorithm;

developed for hyperbolic systems in the past few decades, though treating supersonic and hypersonic combustion problems are non-trivial. Some of the important contributions in modelling multicomponent flows are due to^{14,15,4,7,2,3,37,5,17,18,33,34,35}.

Fernandez *et al.*¹¹, aimed at constructing an efficient conservative numerical scheme for computation of multi-species flows. The governing equations are Euler equations and additional equations for the species with different molecular weights and specific heats are considered. Approximate Riemann solver of Roe has been used and modifications for evaluation of γ in the Roe matrix have been suggested. Donor cell approximation method for species equations is modelled and compared with the modifications of the Roe scheme. They conclude that the modified Roe scheme performs better than the donor cell approximation method.

Larroutourou *et al.*¹⁷, have reviewed various numerical methods for multicomponent perfect and real gas models. They have suggested modifications for Osher, Steger-Warming, van Leer and Roe schemes for the application to multicomponent perfect and real gases. They show clearly that, for multicomponent flows Roe's conditions (consistency, conservation and hyperbolicity) get satisfied only when $\gamma(U)$ is constant and hence the extension of Roe scheme for multicomponent mixture flows is not an easy task.

Karni¹⁴ has carried out modelling of multicomponent fluids using Euler equations with an additional equation for the species. Both conservative and non-conservative form of the equations are considered and primitive form of the equations are recommended to avoid the pressure oscillations occurring near the material interface. Four different models of the governing equations with variable γ and a level set method based on distance function are used in both conservative and primitive form. Roe linearisation method is used in numerical simulation and compared with second order upwind methods. It is concluded that any fully coupled conservative based numerical scheme leads to pressure oscillations and non-preserving of positivity of mass fractions. She recommended the use of primitive variable based approach in order to avoid the pressure oscillations. The use of non-conservative form, however, leads to conservative errors and incorrect shock positions.

Abgrall², has used a quasi-conservative approach for the calculations for multicomponent cases and proved that an additional evolution equation of γ and in particular of the form $\frac{1}{(\gamma-1)}$, is suggested to preserve mass fraction positivity and to avoid pressure oscillations.

Abgrall and Karni⁴ have reviewed numerical algorithms commonly used in the simulations of multicomponent compressible fluid flow. They conclude that if separate equations for individual species are solved along with the mixture equations, then the numerical scheme developed preserves pressure equilibrium and mass fraction positivity.

Keh-Ming Shyue in^{33,34,35,36}, has utilized Abgrall's model² for compressible multicomponent flow problems using stiffened gas EOS, van der Waals EOS, Mie-Gruneisen EOS, Tait EOS.

Overall the basic issues in extending the single fluid conservative numerical schemes to multicomponent flows are

1. preserving the positivity of mass fraction,
2. avoiding pressure oscillations even in the first order numerical scheme,
3. difficulties in extension to more than 2 components.

In this work novel and accurate central solvers MOVERS-n, MOVERS-1, developed by¹² along with MOVERS+, RICCA as explained in²⁷ are applied to multicomponent flows to address some of the above issues.

2 Governing equations for mixture with two components or species

From the literature it is observed that there are many different ways in which the governing equations can be formulated. A simple case of non-reacting mixture equations with two components and without diffusion is considered in the present work. Two models based on mass fraction Y and γ are chosen to test the algorithms in conservative cell centered finite volume frame work. In the following sections the governing equations for these models and basic algorithms used to discretise them are discussed briefly.

2.1 Mass fraction based model

Consider the mixture of gasses consisting of two species with following mixture properties: pressure p , density ρ , velocity u and temperature T . The mixture pressure is given by Dalton's Law $p = p_1 + p_2$, mixture density $\rho = \rho_1 + \rho_2$, the mass fraction of the species $Y_k = \frac{\rho_k}{\rho}$, $k = 1, 2$. Specific heat at constant pressure and constant volume of individual species, c_{p_k}, c_{v_k} , $k = 1, 2$ are considered to be constant, and the ratio of specific heats of individual species is given by $\gamma_k = \frac{c_{p_k}}{c_{v_k}}$, $k = 1, 2$. The governing

equations for the mixture in conservation form are given by (2.1)

$$\left. \begin{aligned} \frac{\partial \rho}{\partial t} + \frac{\partial (\rho u)}{\partial x} &= 0, \\ \frac{\partial \rho u}{\partial t} + \frac{\partial (\rho u^2 + p)}{\partial x} &= 0, \\ \frac{\partial \rho E_t}{\partial t} + \frac{\partial [(\rho E_t + p) u]}{\partial x} &= 0, \\ \frac{\partial (\rho Y_k)}{\partial t} + \frac{\partial (\rho Y_k u)}{\partial x} &= 0, \quad k = 1, 2 \\ Y_1 + Y_2 &= 1 \end{aligned} \right\} \quad (2.1)$$

The value of ratio of specific heats, γ , for the mixture, is defined as $\gamma = \frac{c_{p,mixture}}{c_{v,mixture}} = \frac{\sum_k Y_k \gamma_k c_{vk}}{\sum_k Y_k c_{vk}}$ and the mixture pressure is given by $p = (\gamma - 1)(\rho E_t - \frac{\rho u^2}{2})$. The equation of state for each individual component can be described by a function $p = p(\rho, e)$. These governing equations are represented in compact notation as in the first equation of (2.2) where enthalpy of the mixture is given by $H = E_t + \frac{p}{\rho}$. The ratio of specific heats for the mixture, γ is a function of the conserved variable vector U , as $\gamma = \frac{U_4 \gamma_1 c_{v1} + (U_1 - U_4) \gamma_2 c_{v2}}{U_4 c_{v1} + (U_1 - U_4) c_{v2}} = \gamma(U_1, U_4)$. This property of γ for the mixture plays a role in determining the hyperbolicity of the governing equations. It can also be observed that (2.2) is extension of Euler equations with an additional equations for the mass fraction of individual component gases. Hence if this set of governing equations satisfies the hyperbolicity principle then all the algorithms which are designed for Euler equations can be in principle extended to multicomponent fluids.

$$\frac{\partial U}{\partial t} + \frac{\partial F(U)}{\partial x} = 0 \quad (2.2)$$

$$U = \begin{bmatrix} U_1 \\ U_2 \\ U_3 \\ U_4 \end{bmatrix} = \begin{bmatrix} \rho \\ \rho u \\ \rho E \\ \rho Y_k \end{bmatrix}; F(U) = \begin{bmatrix} \rho u \\ \rho u^2 + p \\ (\rho E + p)u \\ \rho Y_k u \end{bmatrix} = \begin{bmatrix} U_2 \\ \frac{(3-\gamma) U_2^2}{2 U_1} + (\gamma - 1) U_3 \\ \frac{(3-\gamma) U_3 U_2}{2 U_1} - \frac{(\gamma-1) U_2^3}{2 U_1^2} \\ \frac{U_4 U_1}{U_2} \end{bmatrix} \quad (2.3)$$

2.2 Hyperbolicity and eigenstructure for the mixture model

To demonstrate the hyperbolicity of equations (2.2), it is required to evaluate the flux Jacobian matrix, it's eigenvalues and corresponding eigenvectors. The flux Jacobian matrix of the governing equations is given by (2.4)

$$A(U) = \begin{bmatrix} 0 & 1 & 0 & 0 \\ \frac{(\gamma-3) U_2^2}{2 U_1^2} + B & (3-\gamma) \frac{U_2}{U_1} & (\gamma-1) B' & \\ \frac{(\gamma-3) U_3 U_2}{2 U_1^2} + uB + (\gamma-1) \frac{U_2^3}{U_1^3} - \frac{(3-\gamma) U_3}{2 U_1} - \frac{3(\gamma-1) U_2^2}{2 U_1^2} & \frac{(3-\gamma) U_2}{2 U_1} & \frac{(3-\gamma) U_2}{2 U_1} & uB' \\ -\frac{U_4}{U_2} & \frac{-U_4 U_1}{U_2^2} & 0 & \frac{U_2}{U_1} \end{bmatrix} \quad (2.4)$$

It can be observed that the flux Jacobian matrix is a function of γ and its derivatives given by (2.5)

$$\begin{aligned} B &= \frac{p}{(\gamma-1)} \frac{\partial \gamma}{\partial U_1}, \\ B' &= \frac{p}{(\gamma-1)} \frac{\partial \gamma}{\partial U_4}. \end{aligned} \quad (2.5)$$

The flux Jacobian matrix (2.4) in terms of specific total enthalpy of mixture H is given by (2.6).

$$A(U) = \frac{\partial F(U)}{\partial U} = \begin{bmatrix} 0 & 1 & 0 & 0 \\ \frac{(\gamma-3)}{2} u^2 + B & (3-\gamma) u & (\gamma-1) B' & \\ \frac{(\gamma-1)}{2} u^3 + Bu - uH & H - (\gamma-1) u^2 & \gamma u & B'u \\ -Y_1 u & Y_1 & 0 & u \end{bmatrix} \quad (2.6)$$

The eigenvalues of the matrix $A(U)^T$ are $(u + a, u, u, u - a)$, where $a = \sqrt{\frac{\gamma p}{\rho}}$, and the right eigenvectors are

$$r_1 = \begin{bmatrix} 1 \\ u - a \\ H - ua \\ Y_1 \end{bmatrix}, r_2 = \begin{bmatrix} 1 \\ u \\ \frac{u^2}{2} - \frac{B}{(\gamma-1)} \\ 0 \end{bmatrix}, r_3 = \begin{bmatrix} 0 \\ 0 \\ -\frac{B'}{(\gamma-1)} \\ 1 \end{bmatrix}, r_4 = \begin{bmatrix} 1 \\ u + a \\ H + ua \\ Y_1 \end{bmatrix} \quad (2.7)$$

The above system is hyperbolic as eigenvalues are real and the eigenvectors are linearly independent.

2.3 Multicomponent fluid simulations with γ -based model and stiffened gas EOS

In his fundamental work, Abgrall² has quoted that any numerical scheme designed for compressible Euler equations extended to multicomponent flows would generate pressure oscillations. It has also been suggested by the author that use of $\frac{1}{(\gamma-1)}$ as the parameter in the quasi-conservative approach would eliminate the pressure oscillations, this has been demonstrated by Shyue^{33,34,35,36}. For γ based model the mixture equations in 1D are given by (2.8).

$$\begin{aligned} \frac{\partial \rho}{\partial t} + \frac{\partial (\rho u)}{\partial x} &= 0 \\ \frac{\partial \rho u}{\partial t} + \frac{\partial (\rho u^2 + p)}{\partial x} &= 0 \\ \frac{\partial \rho E}{\partial t} + \frac{\partial [(\rho E + p)u]}{\partial x} &= 0 \end{aligned} \quad (2.8)$$

Here, Y^i represent the volume fraction of the component gases in a given cell or control volume and $\rho, u, p, p_\infty, \gamma$ represent the mixture density, mixture velocity, mixture pressure, mixture stiffened pressure and mixture gamma respectively.

$$\frac{\partial \left(\frac{\rho}{(\gamma-1)} \right)}{\partial t} + \frac{\partial \left(\frac{\rho u}{(\gamma-1)} \right)}{\partial x} = 0 \quad (2.9)$$

$$\frac{\partial \left(\frac{\rho \gamma p_\infty}{(\gamma-1)} \right)}{\partial t} + \frac{\partial \left(\frac{\rho \gamma p_\infty u}{(\gamma-1)} \right)}{\partial x} = 0 \quad (2.10)$$

$$\frac{p + \gamma p_\infty}{\gamma - 1} = \rho e \quad (2.11)$$

In the above equations (2.11) refer to stiffened gas EOS. This EOS would revert to perfect gas EOS in the limit $p_\infty \rightarrow 0$. These equations (2.9) along with (2.8) are referred to as γ -based model by Abgrall¹.

2.4 Numerical Methodology and Novel Algorithms

The governing equations are Euler equations in conservative form as given in (2.12a)

$$\frac{d\bar{U}}{dt} = -R, \quad R = \frac{1}{\Omega} \left[\sum_{i=1}^N F_c \cdot \hat{n} dS \right], \quad (2.12a)$$

$$\bar{U} = \frac{1}{\Omega} \int_{\Omega} U d\Omega. \quad (2.12b)$$

where U is conserved variable vector, F_c is convective flux vector on an interface, R representing net flux from a given control volume, Ω volume of control volume and N representing number of control surfaces for a given control volume. The convective flux on any interface of a control volume as shown in figure(1) for any stable scheme can be written as the sum of an average flux across the interface and a numerical dissipative flux as given in (2.13a).

$$F_1 = \frac{1}{2} [F_L + F_R] - d_1 \quad (2.13a)$$

$$d_1 = \frac{|\alpha_1|}{2} (U_R - U_L) \quad (2.13b)$$

where α_1 coefficient of numerical diffusion and d_1 represents the numerical dissipative flux. In the present work the coefficient of numerical diffusion is determined by MOVERS¹², RICCA and MOVERS+²⁷ as briefed in sections(2.4.1,2.4.2 & 2.4.3) are utilised to simulate the mixture equations based on mass fraction model with perfect gas EOS and γ based model with stiffened gas EOS. These algorithms are independent of eigenstructure of the underlying hyperbolic system and can be extended to any arbitrary EOS.

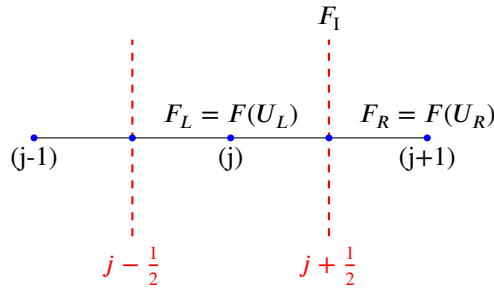


FIGURE 1 Typical finite volume in 1D

2.4.1 MOVERS

The central scheme of interest is due to ¹² who introduced a new central scheme named MOVERS (*Method of Optimal Viscosity for Enhanced Resolution of Shocks*) which can capture grid aligned shocks and contact-discontinuities accurately. This coefficient of numerical diffusion rewritten in terms of RH conditions is given by (2.14)

$$|\alpha_I|_i = |s_i| = \left| \frac{\Delta F_i}{\Delta U_i} \right|, \quad i = 1, 2, 3, \quad \Delta(\cdot) = (\cdot)_R - (\cdot)_L \quad (2.14)$$

In order to introduce boundedness and further stabilize the numerical scheme, α_I is to be restricted to a physically feasible range of eigenvalues of the flux Jacobian matrix. This process known as wave speed correction (2.15) is incorporated such that the coefficient of numerical diffusion lies within the eigenspectrum of the flux Jacobian *i.e.*, $\alpha_I \in [\lambda_{max}, \lambda_{min}]$.

$$|\alpha_I| = \begin{cases} \lambda_{max}, & \text{if } |\alpha_I| > \lambda_{max} \\ \lambda_{min}, & \text{if } |\alpha_I| < \lambda_{min} \\ |\alpha_I|, & \text{otherwise} \end{cases} \quad (2.15)$$

This method is independent of eigenstructure of the underlying hyperbolic systems, is simple and can capture grid-aligned stationary discontinuities exactly. Authors ¹² introduced two variations of MOVERS: (i) an n -wave based coefficient of numerical diffusion, corresponding to n number of conservation laws (MOVERS- n) and (ii) a scalar diffusion, corresponding to the energy equation, referred to as MOVERS-1. The robustness of the basic scheme has been improvised through its variants by Maruthi N.H. ²⁵ and extended them to hyperbolic systems for magnetohydrodynamics and shallow water flows. In this work this algorithm is chosen as the foundation to devise two new efficient algorithms for hyperbolic systems. The simplicity and accuracy of this algorithm make this scheme a well-suited base-line solver for further research, apart from its independency of the eigenstructure.

2.4.2 Riemann Invariant based Contact-discontinuity Capturing Algorithm (RICCA)

The numerical diffusion evaluated using Riemann Invariant based Contact-discontinuity Capturing Algorithm (RICCA) is given by

$$\alpha_I = \begin{cases} \frac{|V_{nL}| + |V_{nR}|}{2}, & \text{if } |\Delta \mathbf{F}| < \delta \text{ and } |\Delta \mathbf{U}| < \delta \\ \max(|V_{nL}|, |V_{nR}|) + \text{sign}(|\Delta p_I|) a_I, & \text{otherwise} \end{cases} \quad (2.16)$$

where $a_I = \sqrt{\frac{\gamma p_I}{\rho_I}}$ is the speed of sound evaluated with the values at the interface given by

$$\rho_I = \frac{\rho_L + \rho_R}{2}, \quad p_I = \frac{p_L + p_R}{2}, \quad \Delta p_I = (p_R - p_L). \quad (2.17)$$

2.4.3 MOVERS without wave speed correction - MOVERS+

The coefficient of numerical diffusion for MOVERS+ is given by

$$|d_1|_j = \Phi \text{Sign}(\Delta U_j) |\Delta F_j| + \left(\frac{|V_{nL}| + |V_{nR}|}{2} \right) \Delta U_j, \quad j = 1, 2, 3 \quad (2.18)$$

These two new algorithms RICCA and MOVERS+

- can capture steady contact-discontinuities exactly,

- has sufficient numerical diffusion near shocks so as to avoid shock instabilities, and
- does not need entropy fix for at sonic points.

A similar strategy was introduced by N.Venkata Raghavendra in^{41,42} to design an accurate contact-discontinuity capturing discrete velocity Boltzmann scheme for inviscid compressible flows.

2.5 Modifications of upwind methods for multicomponent flows

As mentioned before, the application of upwind methods to multicomponent flows is non-trivial because these methods are strongly dependent on the eigenstructure. Larrourou and Fezoui¹⁷ have reviewed these modifications needed for upwind methods, which are briefly presented here.

2.5.1 Extension of Steger-Warming FVS method to multicomponent gases

The Flux Vector Splitting (FVS) method of Steger-Warming method as given in⁹, leads to the following split flux vectors for Euler equations.

$$F^{\pm} = \frac{\rho}{2\gamma} \begin{bmatrix} (u-a)\lambda_1^{\pm} + 2(\gamma-1)\lambda_2^{\pm} + \lambda_3^{\pm} \\ \lambda_1^{\pm} + 2(\gamma-1)u\lambda_2^{\pm} + (u+a)\lambda_3^{\pm} \\ (H-ua)\lambda_1^{\pm} + 2(\gamma-1)u^2\lambda_2^{\pm} + (H+ua)\lambda_3^{\pm} \end{bmatrix} \quad (2.19)$$

For the mixture equations (2.1), an additional fourth component (for the extra mass fraction term) for the split flux vectors is given by

$$F[4] = \rho u Y_1 = F^{\pm}[1] Y_1. \quad (2.20)$$

2.5.2 Extension of van Leer FVS method to multicomponent gases

The details of the flux vector splitting developed by van Leer are given in⁹ for Euler equations. Extension of van Leer flux splitting to multicomponent mixture equations as a function of Mach number is given by

$$F = F(\rho, a, M, Y) = \begin{bmatrix} \rho a M \\ \rho a^2 (M^2 + 1) \\ \rho a^3 M \left(\frac{M^2}{2} + \frac{1}{\gamma-1} \right) \\ \rho a M Y_1 \end{bmatrix} \quad (2.21)$$

The split fluxes given in¹⁷ are

$$F^{\pm} = \frac{1}{4} \rho a (1 \pm M)^2 \begin{bmatrix} 1 \\ \frac{2a}{\gamma} \left(\frac{\gamma-1}{2} M \pm 1 \right) \\ \frac{2a^2}{\gamma^2-1} \left(\frac{\gamma-1}{2} M \pm 1 \right)^2 \\ Y_1 \end{bmatrix} \quad (2.22)$$

2.5.3 Extension of Roe's FDS method

Roe's Flux Difference Splitting (FDS) method, which is an approximate Riemann solver, cannot be directly extended to multicomponent flows in a trivial way. In order to evaluate Roe's numerical flux, the following information is necessary

- wave strengths $\tilde{\alpha}_i$,
- eigenvalues of the flux Jacobian matrix $\tilde{\lambda}_i$,
- right eigenvectors of the flux Jacobian matrix $\tilde{R}^{(i)}$.

The following basic conditions (also called as U property) are to be satisfied by Roe scheme

1. consistency, $A(U_L, U_R) = A(U)$ if $U_L = U_R = U$,
2. hyperbolicity *i.e.*, flux Jacobian matrix should have real eigenvalues,
3. conservation across discontinuities, $F(U_R) - F(U_L) = A(U_R - U_L)$.

The two component scheme for the interface flux given in¹⁷ is

$$F(U_L, U_R) = \frac{1}{2} (F(U_L) + F(U_R)) + \frac{1}{2} |\tilde{A}| (U_L - U_R) \quad (2.23)$$

where U represents the average state between the left and right states. The averaged state is defined as

$$\left. \begin{aligned} U &= [\tilde{\rho}, \tilde{\rho}\tilde{u}, \tilde{\rho}\tilde{E}, \tilde{\rho}\tilde{Y}]^T \\ \tilde{\rho} &= \frac{\rho_L\sqrt{\rho_L} + \rho_R\sqrt{\rho_R}}{\sqrt{\rho_L} + \sqrt{\rho_R}} \\ \tilde{u} &= \frac{u_L\sqrt{\rho_L} + u_R\sqrt{\rho_R}}{\sqrt{\rho_L} + \sqrt{\rho_R}} \\ \tilde{H} &= \frac{H_L\sqrt{\rho_L} + H_R\sqrt{\rho_R}}{\sqrt{\rho_L} + \sqrt{\rho_R}} \\ \tilde{Y} &= \frac{Y_L\sqrt{\rho_L} + Y_R\sqrt{\rho_R}}{\sqrt{\rho_L} + \sqrt{\rho_R}} \end{aligned} \right\} \quad (2.24)$$

$$\tilde{A}(U) = \begin{bmatrix} 0 & 1 & 0 & 0 \\ \frac{(\tilde{\gamma}-3)}{2}\tilde{u}^2 + \tilde{B} & (3-\tilde{\gamma})\tilde{u} & (\tilde{\gamma}-1)\tilde{B}' & \\ \frac{(\tilde{\gamma}-1)}{2}\tilde{u}^3 + \tilde{B}\tilde{u} - \tilde{u}\tilde{H} & \tilde{H} - (\tilde{\gamma}-1)\tilde{u}^2 & \tilde{\gamma}\tilde{u} & \tilde{B}'\tilde{u} \\ -\tilde{Y}_1\tilde{u} & \tilde{Y}_1 & 0 & \tilde{u} \end{bmatrix}$$

The matrix \tilde{A} as given in (2.24) is diagonalisable, and its eigenvalues, as given in⁷, are $(\tilde{u} - \tilde{a}, \tilde{u}, \tilde{u}, \tilde{u} + \tilde{a})$ where $(\tilde{a}^2 = (\tilde{\gamma}-1)\left(\tilde{H} - \frac{\tilde{u}^2}{2}\right))$.

The following remarks are given in^{7,5}, which highlights the conditions under which Roe scheme is not applicable.

Remark 1. For two component fluid flow, the conservation property is satisfied only if $\gamma_1 = \gamma_2 = \text{Constant}$. If $\gamma_1 \neq \gamma_2$, then pressure oscillations are observed in the case of steady contact discontinuities.

Remark 2. In order to satisfy the conservation property $\tilde{A}(U)$ has to be modified to $A(\tilde{U})$, for which the following definitions of $\tilde{B}' = \frac{c_{v1}c_{v2}(\gamma_1-\gamma_2)\tilde{T}}{\tilde{Y}_1c_{v1}+(1-\tilde{Y}_1)c_{v2}}$ and $\tilde{T} = \frac{T_L\sqrt{\rho_L}+T_R\sqrt{\rho_R}}{\sqrt{\rho_L}+\sqrt{\rho_R}} \neq T(\tilde{U})$ are used. The Jacobian matrix \tilde{A} is diagonalisable only if this modification is incorporated.

Remark 3. This expression $\tilde{B}' = \frac{c_{v1}c_{v2}(\gamma_1-\gamma_2)\tilde{T}}{\tilde{Y}_1c_{v1}+(1-\tilde{Y}_1)c_{v2}}$ is not easily extendable to a mixture of more than 2 components.

Remark 4. If the two states U_L and U_R are supersonic and satisfy $u_L \geq a_L, u_R \geq a_R$, and when using upwind schemes, the flux $\phi(U_L, U_R) = F(U_L)$, is satisfied in all upwind schemes, modified for multicomponent cases, except for Roe scheme.

Remark 5. The construction of Jacobian matrix of average the state $\tilde{A}(U_L, U_R) = A(\tilde{U})$, is impossible for a complex equation of state for multicomponent cases.

It can be observed that direct extension of Roe scheme to multicomponent fluids is not an easy task. The new central solvers introduced in section(2.4.1,2.4.2,2.4.3), RICCA and MOVERS+, along with MOVERS-1 and MOVERS-n, do not require any of the above modifications as they are not dependent on eigenstructure at all.

3 Results for mass fraction based model

In this section the test cases used for the validation of the central solvers, MOVERS-1, MOVERS-n, MOVERS+ and RICCA, for multicomponent flows are discussed. Initial conditions for the 1-D shock tube are given in table (2).

Test case	ρ_L	H_L	u_L	ρ_R	H_R	u_R	γ_L	γ_R	Time
1	1.0	1.0	0.0	0.125	1.0	0.0	1.4	1.6	steady case

TABLE 1 Steady contact-discontinuity test case with perfect gas EOS

Test case	ρ_L	p_L	u_L	ρ_R	p_R	u_R	γ_L	γ_R	Time
1	1.0	1.0	-1.0	1.0	5.0	1.0	1.4	1.4	0.21
2	1.0	1000.0	0.0	0.125	1.0	0.0	1.6	1.4	0.21

TABLE 2 Initial conditions for shock tube problem and mass fraction positivity test case: data obtained from^{14, 7} with Perfect gas EOS

A fully coupled approach is used for the flux evaluation approach as explained in⁷ and it is stated that the Steger-Warming scheme and van Leer Scheme will preserve the maximum of $0 \leq Y \leq 1$ as they are using a fully coupled approach.

3.1 Steady contact-discontinuity

This test case refers to a contact discontinuity wherein there is a jump in density and γ as given in table (1). The shock tube is filled with two different perfect gases denoted by variable γ . The initial discontinuity is present at $x = 0.5$ with $x \in [0, 1]$. A total of 100 control volumes are used in simulations. Various numerical schemes like Steger Warming, VanLeer, MOVERS-n, MOVERS-1, RICCA and MOVERS+ are compared for this test case. The ability of the numerical schemes to resolve the steady contact-discontinuity is analysed here.

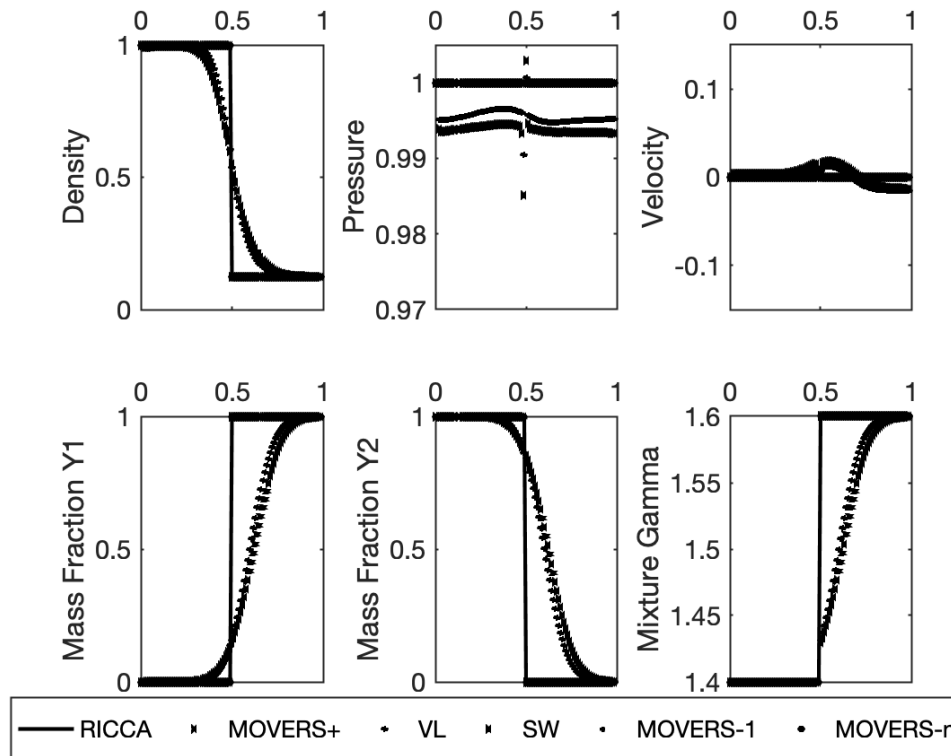


FIGURE 2 Steady contact-discontinuity Comparison of RICCA, MOVERS+, MOVERS-n, MOVERS-1, Vanleer and Steger Warming with unequal γ

Figures (2) refer to comparison of solution obtained for the steady contact-discontinuity case as given in table (1). It can be observed that RICCA, MOVERS+, MOVERS-1 and MOVERS-n resolve the steady contact exactly and even the mass fraction is resolved exactly, whereas for Steger-Warming and van Leer methods, the contact discontinuity and the mass fractions are diffused. It can also be observed that in Steger-Warming scheme and van Leer scheme oscillations are present in pressure and velocity but the positivity of the mass fraction is preserved.

3.2 Pressure oscillations test case

This test case (2) is used by¹⁵, to test the positivity of the mass fraction by the regular Godunov type conservative finite volume methods. In¹⁵, the authors claim that many of the numerical methods which are formulated in the conservative finite volume method would fail to preserve the positivity of the mass fraction. Further, the pressure and velocity have oscillations for the regular finite volume methods. Figures (3) refer to isolated material front test case as described in table (2). As commented

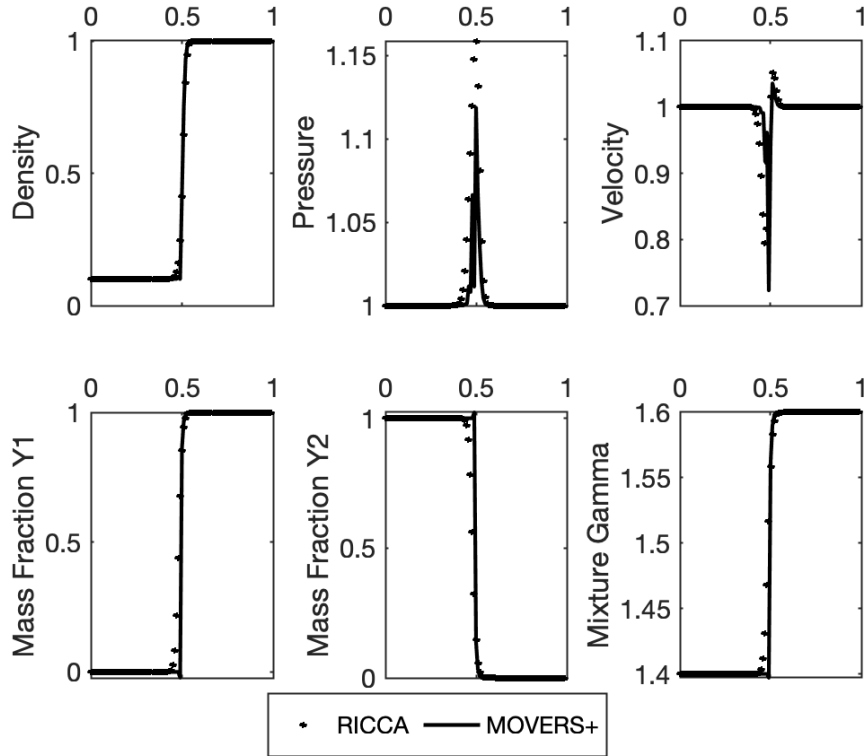


FIGURE 3 Isolated material front problem using RICCA and MOVERS+

by the authors in⁴, for this test case pressure oscillations are present for all first-order numerical schemes which are designed based on the conservative formulation with fully coupled approach and the positivity of the mass fractions for such scheme is doubtful. Though the new algorithms are based on a fully coupled approach in conservative formulation with controlled numerical diffusion, they produce mild oscillations in pressure but they preserve the positivity of the mass fraction unlike the other conservative schemes.

3.3 Sod shock tube test case

This is a standard test case whose initial conditions are given in table (2) for variable gamma values. The data values of the test case are taken from¹⁴ also referred in⁷. The second test case is a stiffer shock tube problem with variation of pressure, mentioned as in test case 3 in table (2). For these shock tube problems the initial discontinuity is located at $x = 0.5$, with mass fraction to the left of the discontinuity $Y_L = 1, Y_R = 0$ and to the right of the discontinuity $Y_L = 0, Y_R = 1$. In all of the computations 100 equally spaced control volumes on the interval $[0, 1]$ are considered with CFL of 0.45 till the prescribed time is reached. Numerical results are presented for Steger-Warming scheme, van Leer scheme, MOVERS-1, MOVERS-n, MOVERS+, and RICCA.

Figures (4) refer to the standard Sod shock tube problem whose initial conditions are defined as test case 2 in table (2). This shock tube problem has two different fluids with different γ values initially separated by a diaphragm placed at $x = 0.5$. Numerical simulations are carried out with 100 control volumes for all schemes and the reference solution is generated using 10000 control volumes using Rusanov Method. Figures (5) refer to the stiff shock tube whose initial conditions are defined

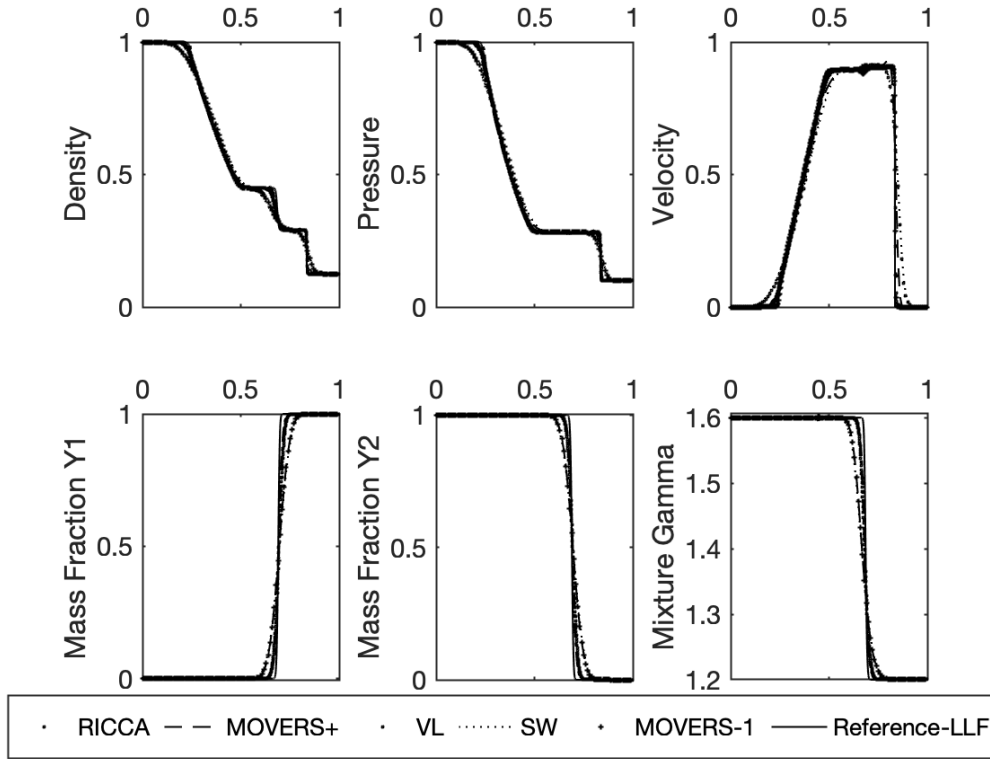


FIGURE 4 Sod shock tube problem using RICCA with unequal γ , $\gamma_L = 1.6$, $\gamma_R = 1.2$

as in test case 3 in table (2). As can be seen all the numerical schemes preserve the mass fraction positivity and no pressure oscillations are present in the pressure.

3.4 1D results for γ -based model

Numerical simulations have been carried out for the test cases described in³³ whose initial conditions are given in the table (3).

Sno	ρ_L	p_L	u_L	ρ_R	p_R	u_R	γ_L	γ_R	$p_{\infty L}$	$p_{\infty R}$	Time
1	1.0	1.0	1.0	0.125	1.0	1.0	1.4	1.2	0	0	0.12
2	1.0	1.0	1.0	0.125	1.0	1.0	1.4	4.0	0	1	0.12
3	1.241	2.753	0.0	1.0	3.059×10^{-4}	0.0	1.4	5.5	0	1.505	0.1
4	1.0	1.0	0.0	5.0	1.0	0.0	1.4	4.0	0	1	0.2
				7.093	10.0	-0.7288		4.0	0	1	0.2

TABLE 3 1D Shock tube test cases referred from³³ with stiffened gas EOS

Test case 1 is an interface only problem and consists of a single contact discontinuity. This test case consists of two sets of data

1. a polytropic gas with two constants states as case 1,
2. has same states except for the changes in γ and P_{∞} as in case 2.

Initial position of the diaphragm is located at $x = 0.2$ and the length of the shock tube, $L = 1$. Results are shown for 10 RICCA and MOVERS+. 100 control volumes are considered for computation for both cases and the results are shown at the prescribed time of 0.12. Figures (6,??) refer to interface only problem with $p_{\infty} = 0$, which corresponds to perfect gas EOS using RICCA and MOVERS+. It can be observed from the figures that the pressure oscillations are not present when gamma based model (unlike in Figure (2.8)) is used and $\frac{1}{\gamma-1}$ is used as the conservative variable as suggested by² and reconfirmed by³³. Shyue has

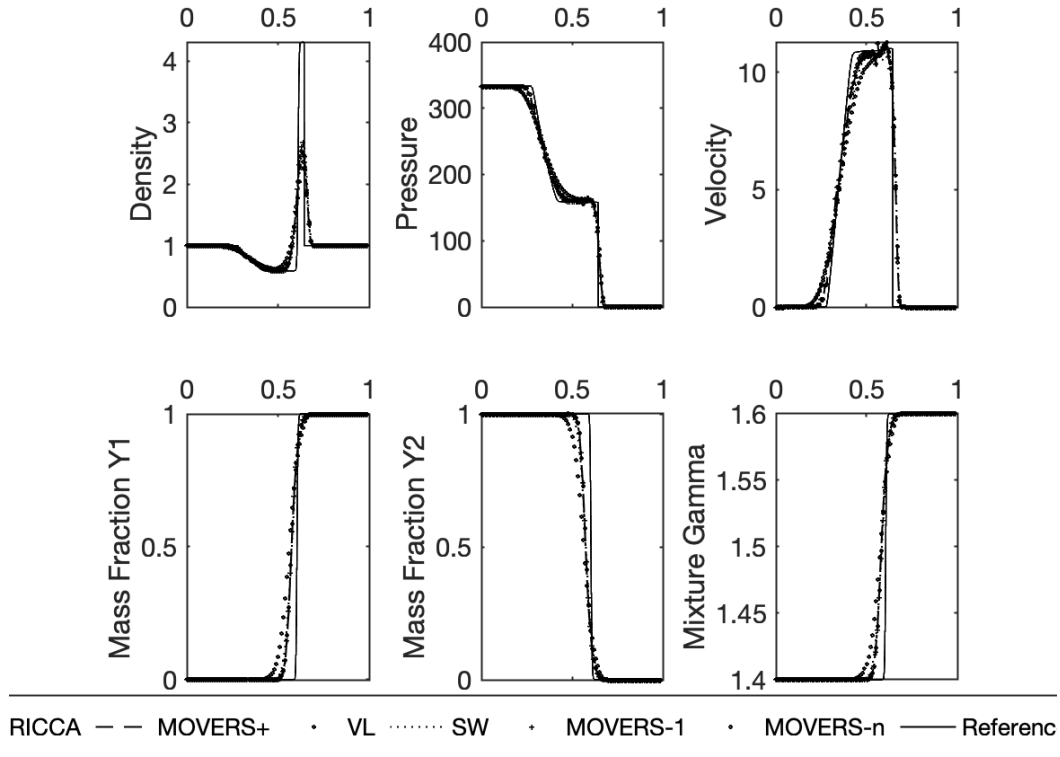


FIGURE 5 Stiff shock tube problem using RICCA,MOVERS+, MOVERS-n,MOVERS-1 with equal gamma $\gamma = 1.4$

also suggested that using eq(10) in³³ cannot be generalised to all shock interaction problems. Figures (7,??) refer to interface only problem with $P_\infty \neq 0$, which corresponds to stiffened gas EOS using RICCA and MOVERS+ schemes. It can be observed from the figure that the pressure oscillations are not present when gamma based model. Even for a large jump in γ both the numerical schemes do not generate any pressure oscillations.

Test case 2 is a two fluid gas-liquid Riemann problem with initial conditions as given in case 3 in the table. The diaphragm position is located with gas occupying the domain till $x \leq 0.5$ and then the liquid and the time for computation is $t = 0.1$. In these test cases the conservative formulation using $\frac{\rho}{\gamma-1}$ is used. Data for reference solution is taken from³³. Simulations are shown for MOVERS+ and RICCA with 100 control volumes. It can be observed from the figures (??,8) and figure (??) that there are no pressure oscillations present in the pressure and the velocity. The internal energy and the p_∞ are accurately predicted.

The third test case considered here is a shock contact-discontinuity interaction problem with the data given as in case 4. Here the two liquids are separated by the interface at $x = 0.5$ and a shock wave located at $x = 0.6$ with the pre- and post-shock conditions as given in the table 3 and the computations are carried out for a time $t = 0.2$. For this case 200 control volumes are considered in the computation, the results from computation are shown in figure (9). It can be seen that the phenomenon is captured accurately by both RICCA and MOVERS+.

3.5 Extension to two dimensions

In this section, the multicomponent model described in the previous section is extended to 2D. The governing equations for γ -based model in 2D are given by (3.1)

$$\frac{\partial \rho}{\partial t} + \frac{\partial (\rho u)}{\partial x} + \frac{\partial (\rho v)}{\partial y} = 0 \quad (3.1)$$

$$\frac{\partial \rho u}{\partial t} + \frac{\partial (\rho u^2 + p)}{\partial x} + \frac{\partial (\rho uv)}{\partial y} = 0 \quad (3.2)$$

$$\frac{\partial \rho v}{\partial t} + \frac{\partial (\rho uv)}{\partial x} + \frac{\partial (\rho v^2 + p)}{\partial y} = 0 \quad (3.3)$$

$$\frac{\partial \rho E_t}{\partial t} + \frac{\partial [(\rho E_t + p) u]}{\partial x} + \frac{\partial [(\rho E_t + p) v]}{\partial y} = 0 \quad (3.4)$$

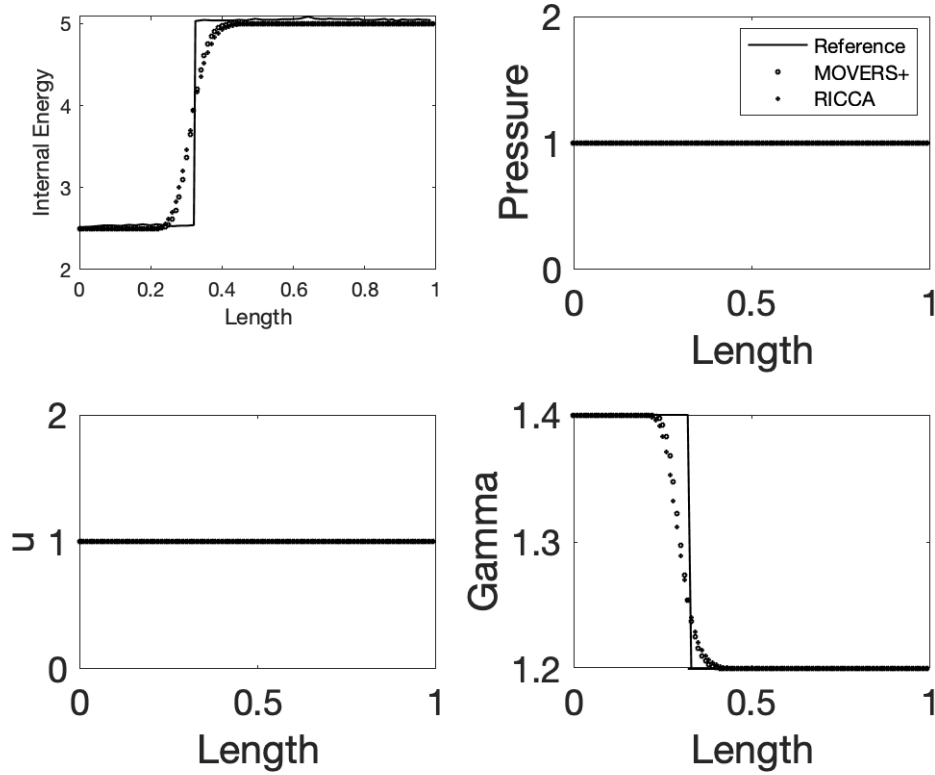


FIGURE 6 Interface only problem with $P_\infty = 0$ simulated using MOVERS+ and RICCA using eq(10) in³³

with the equations γ given by

$$\frac{\left(\frac{\partial \rho}{(\gamma-1)}\right)}{\partial t} + \frac{\left(\frac{\partial \rho u}{(\gamma-1)}\right)}{\partial x} + \frac{\left(\frac{\partial \rho v}{(\gamma-1)}\right)}{\partial x} = 0 \quad (3.5)$$

$$\frac{\left(\frac{\partial \rho \gamma P_\infty}{(\gamma-1)}\right)}{\partial t} + \frac{\left(\frac{\partial \rho \gamma P_\infty u}{(\gamma-1)}\right)}{\partial x} + \frac{\left(\frac{\partial \rho \gamma P_\infty v}{(\gamma-1)}\right)}{\partial y} = 0 \quad (3.6)$$

and stiffened gas EOS as given by (3.7).

$$\frac{p + \gamma P_\infty}{\gamma - 1} = \rho e \quad (3.7)$$

For the 2D γ -based model given above, simulations are carried out using RICCA and MOVERS+.

3.5.1 Moving Interface Problem

The first test case considered is a moving interface problem which consists of a bubble with radius $r_0 = 0.16$ evolving in a constant velocity field $(u, v) = (1, 1)$. The initial data considered here is similar to the 1D test case as described in table (3). The pressure is uniform with value $p = 1$ while the ρ, γ, p_∞ jump across the interface. Initially the bubble is placed at $x_c = 0.25, y_c = 0.25$ on a domain which varies from $x \in [0, 1]$ and $y \in [0, 1]$. A total of 100×100 control volumes are considered in x and y directions and the solution is evolved using a time accurate scheme till $t = 0.36$.

Figure (13) refers to the moving bubble at $t = 0$ and at $t = 0.36$ using RICCA and MOVERS+ on a 100×100 grid and Figure (17) refers to results obtained on a 500×500 grid. It can be observed that the position of the bubble is captured accurately and the pressure does not have any oscillations. Further the pressure and density plots across the bubble are shown in the figure (20) where in it can be observed that there are no pressure oscillations in the results generated by both RICCA and MOVERS+.

3.5.2 Bubble explosion problem

The second test case considered is a radially symmetric problem. It consists of a circular bubble present initially at rest in water and suddenly explodes due to high pressure of the water. The bubble is placed at $(x, y) = (0.5, 0.5)$ and has a radius of

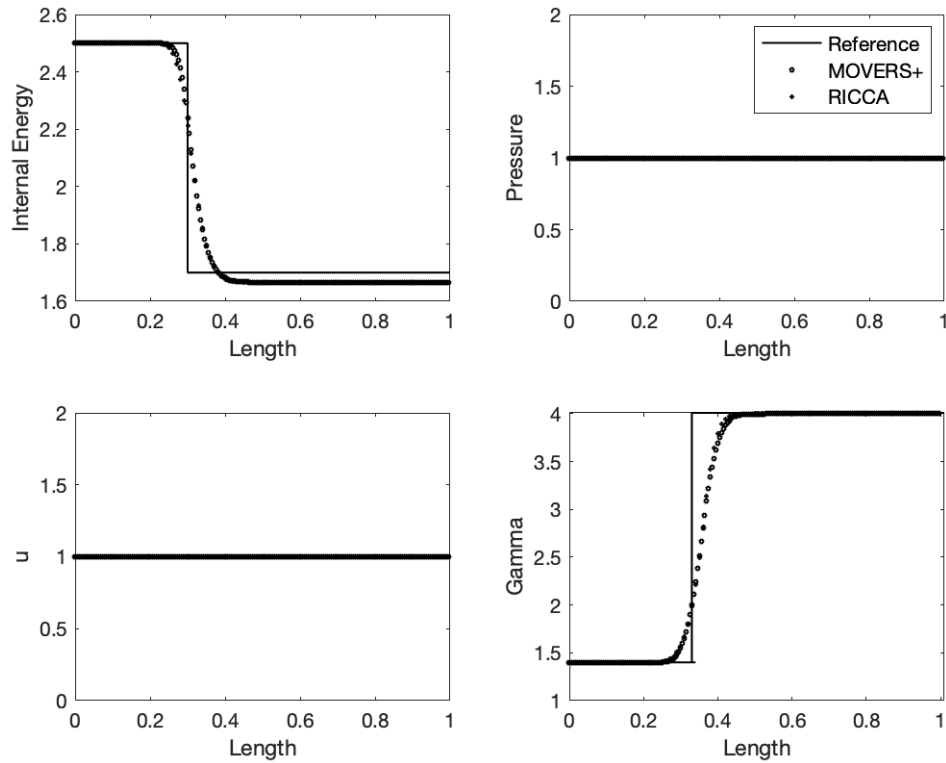


FIGURE 7 Interface only problem with stiff gas simulated using RICCA using eq(10) of³³

$r_o = 0.2$. The fluid inside the bubble has the following initial conditions $(\rho, p, \gamma, p_\infty) = (1.241, 2.753, 1.4, 0)$ and the surrounding water has the following properties $(\rho, p, \gamma, p_\infty) = (0.991, 3.059 \times 10^{-4}, 5.5, 1.505)$. Numerical simulations are carried out using RICCA and MOVERS+. Pressure and density contour plots are shown in figure (24) and the variation of pressure and density at $y = 0.5$ are shown in figure (25).

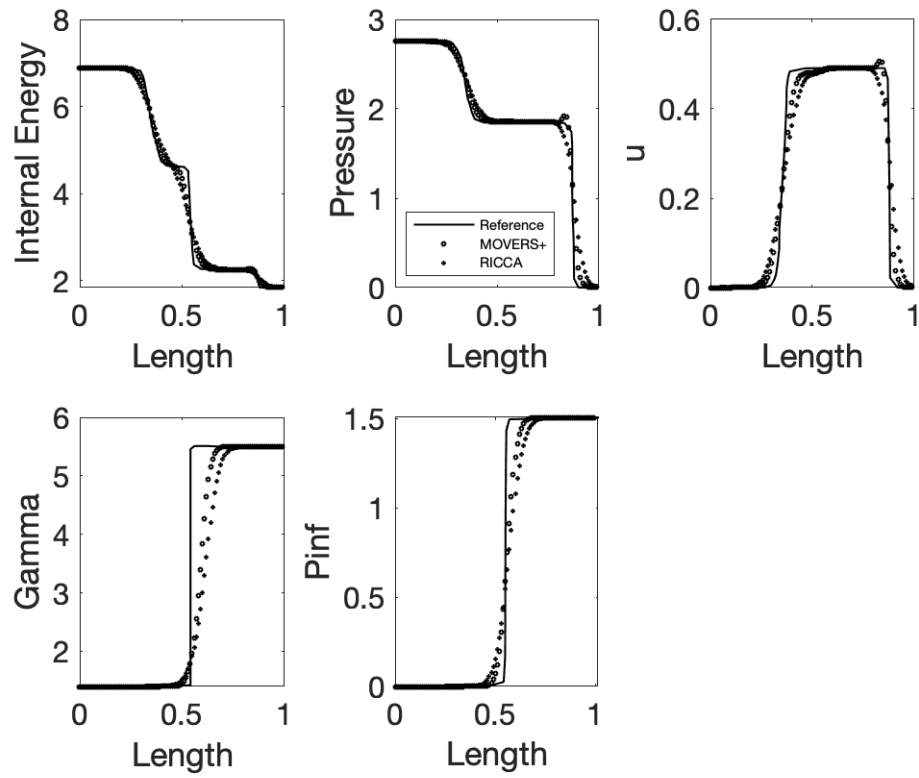


FIGURE 8 Liquid gas Riemann problem using MOVERS+ and RICCA

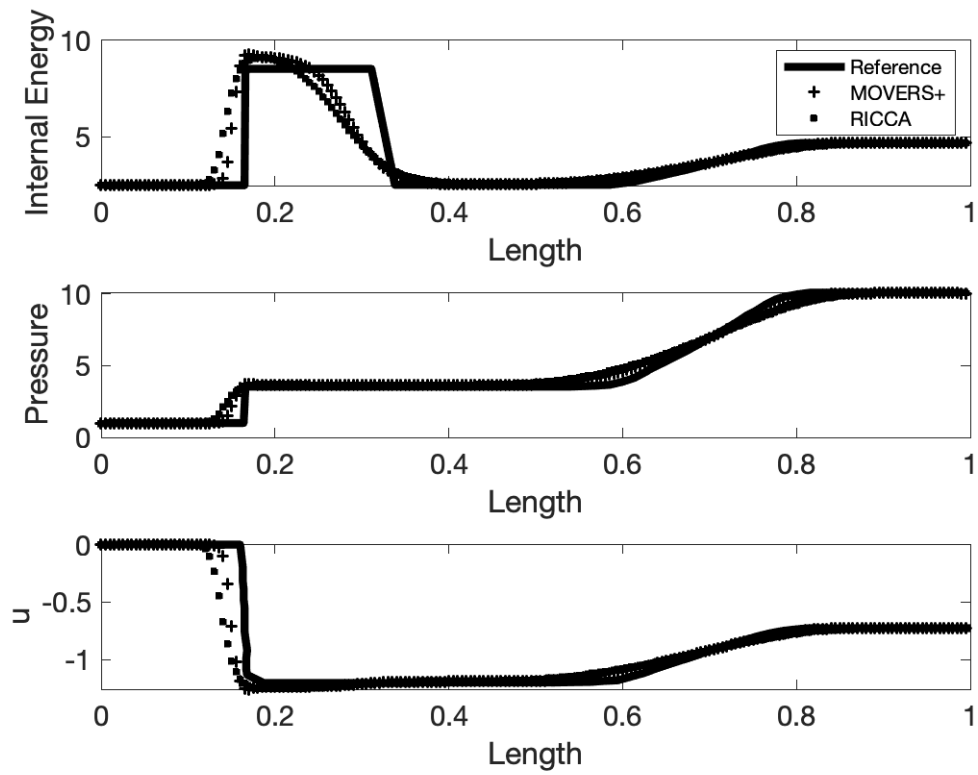


FIGURE 9 Sock contact interaction problem using RICCA and MOVERS+

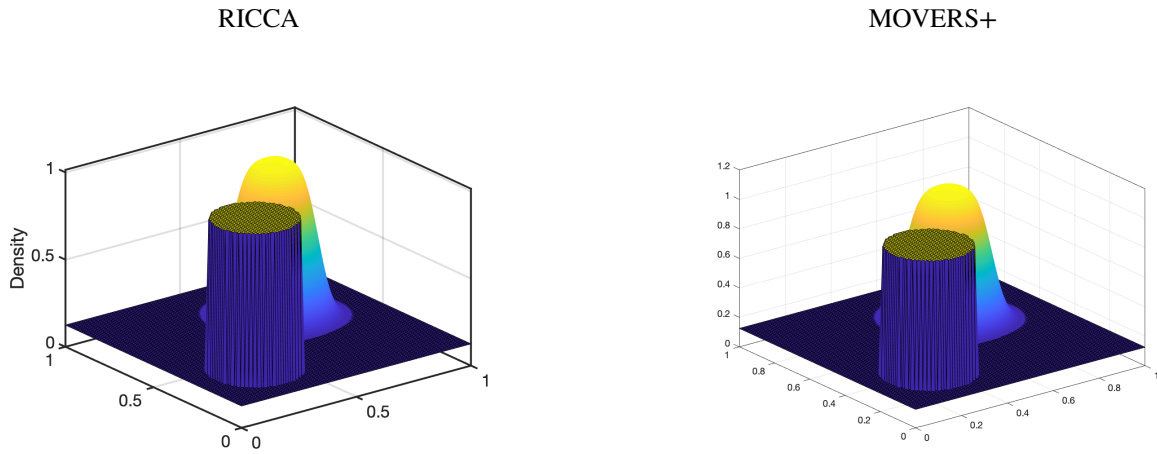


FIGURE 10 Surface of density at $t = 0$ and $t = 0.36$

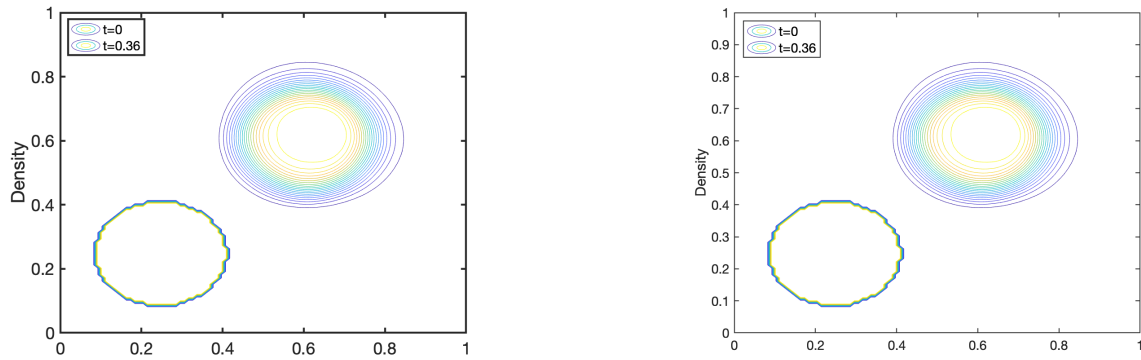


FIGURE 11 Density contours at $t = 0$ and $t = 0.36$

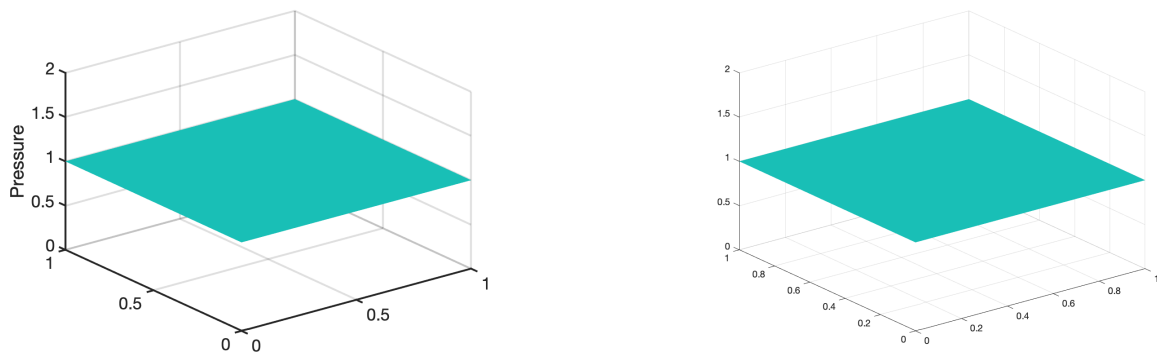


FIGURE 12 Pressure distribution in the domain

FIGURE 13 Contour and surface view of density and pressure of interface only at $t = 0.36$ on 100×100 Grid

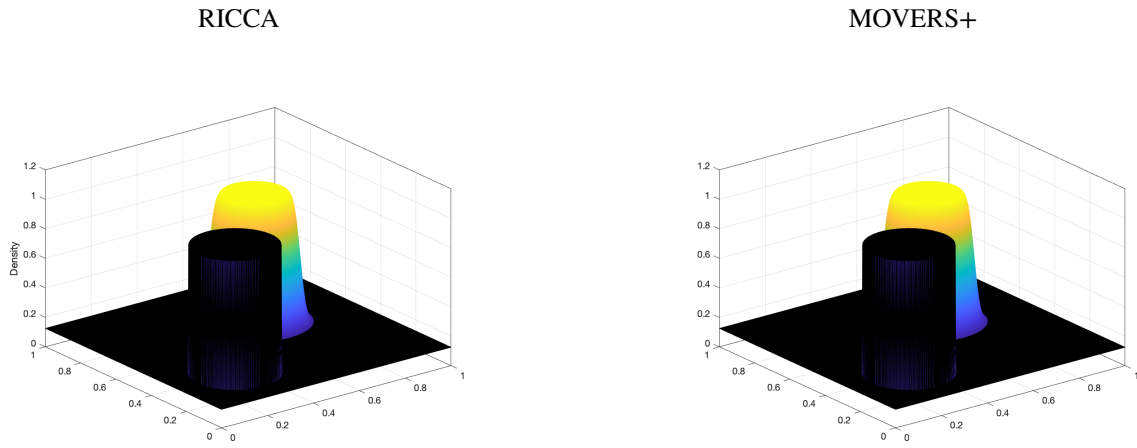


FIGURE 14 Surface of density at $t = 0$ and $t = 0.36$

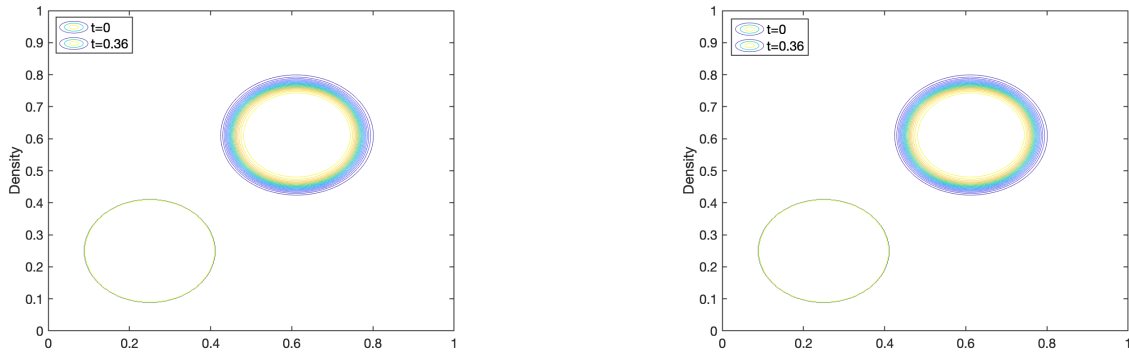


FIGURE 15 Density contours at $t = 0$ and $t = 0.36$

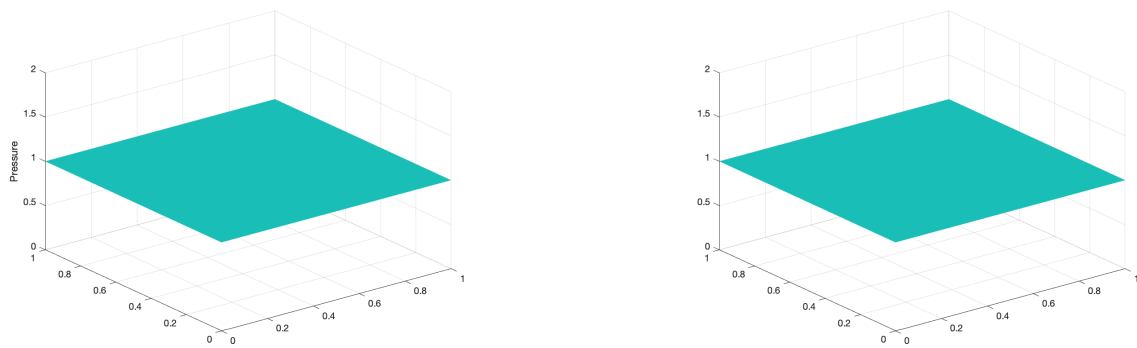


FIGURE 16 Pressure distribution in the domain

FIGURE 17 Contour and surface view of density and pressure of interface only at $t = 0.36$ on 500×500 Grid

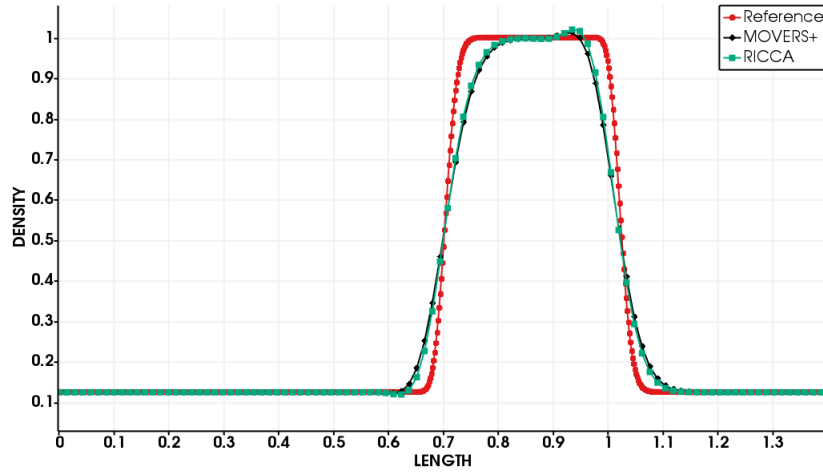


FIGURE 18 Line plot of density across the interface

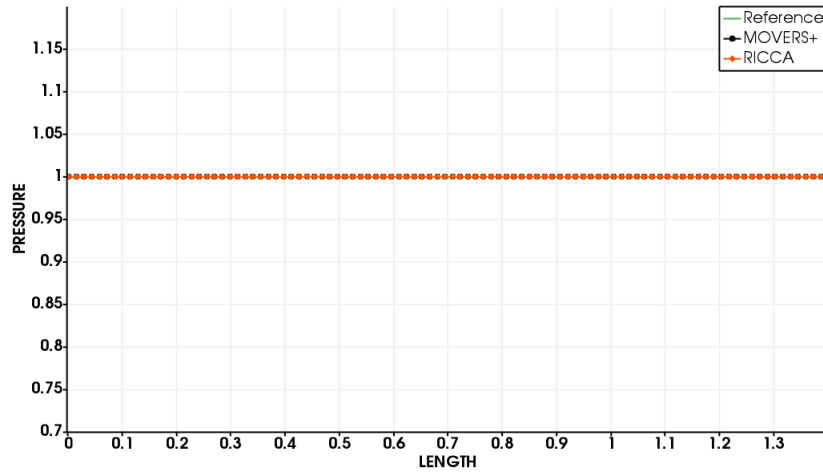


FIGURE 19 Line plot of pressure across the interface

FIGURE 20 2D Line plots of density and pressure across the interface using RICCA Scheme on 500×500 and 100×100 Grid

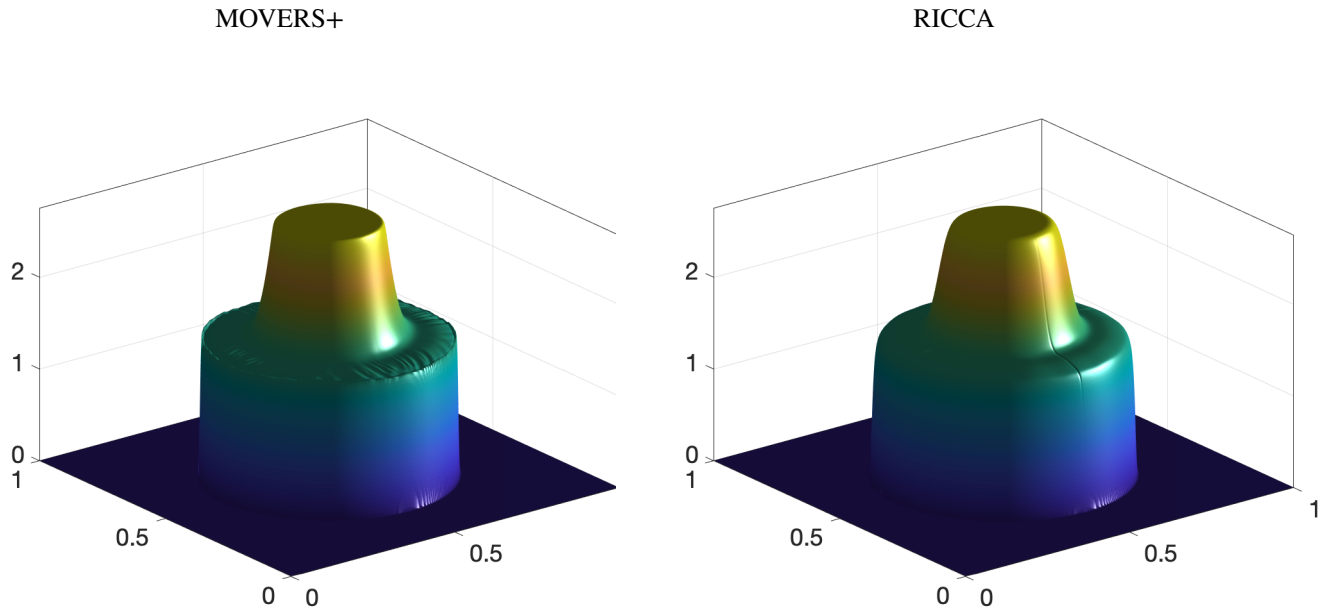


FIGURE 21 Surface pressure of bubble explosion

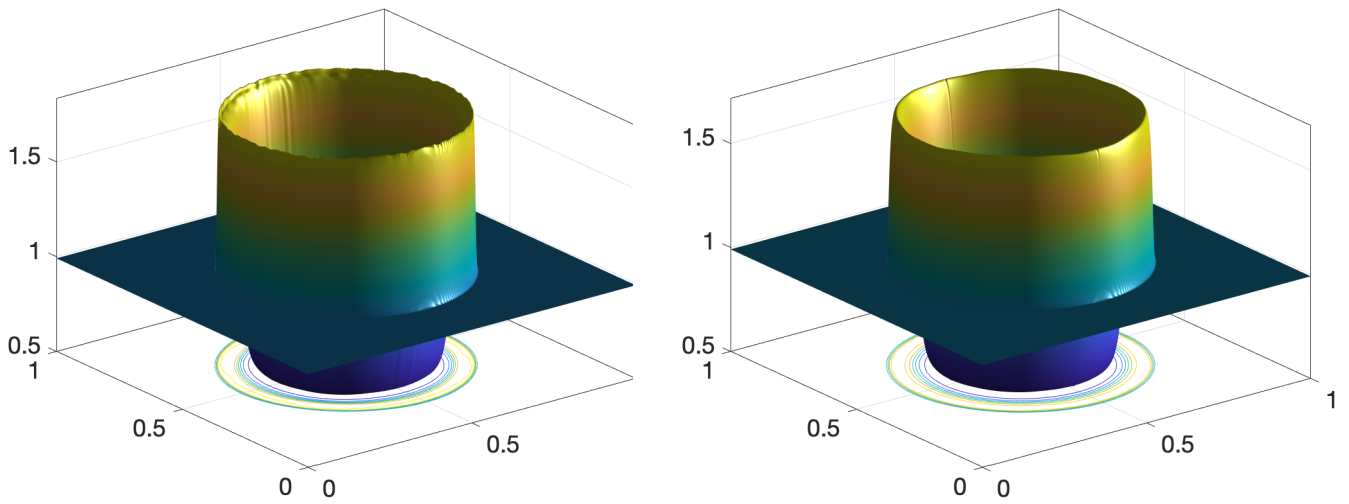


FIGURE 22 Surface density of bubble explosion

FIGURE 23 Contour and surface view of density and pressure of bubble explosion under water at $t = 0.058$ using MOVERS+ and RICCA on 500×500 Grid

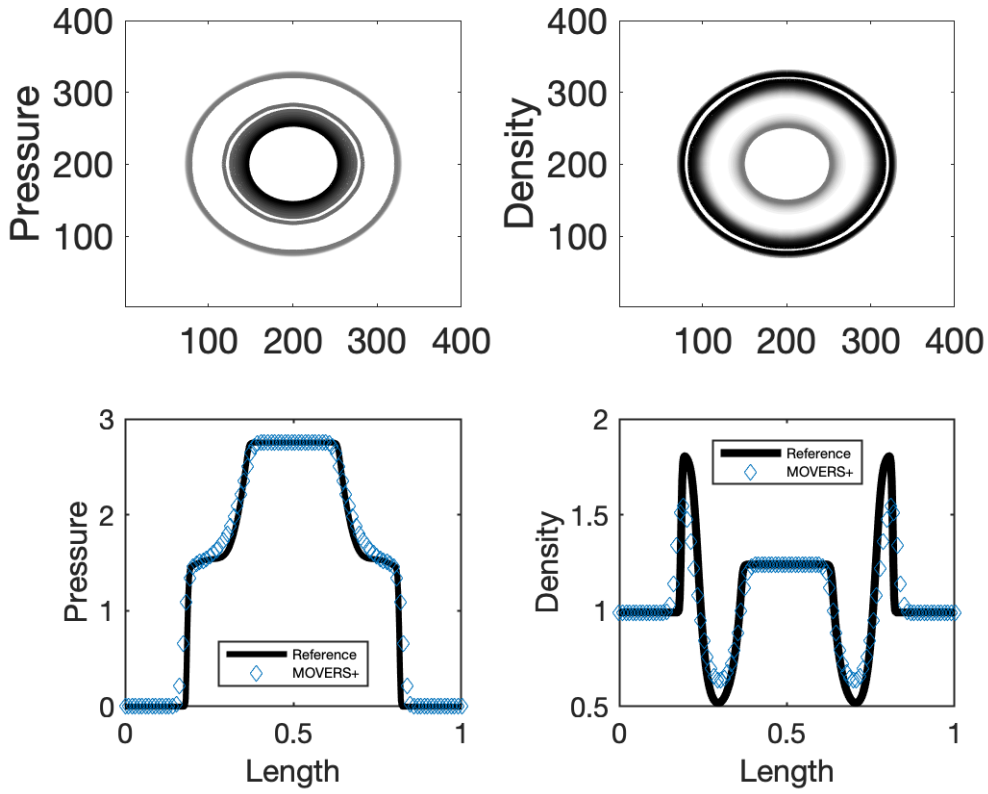


FIGURE 24 2D Line and contour plots of density and ressure using MOVERS+

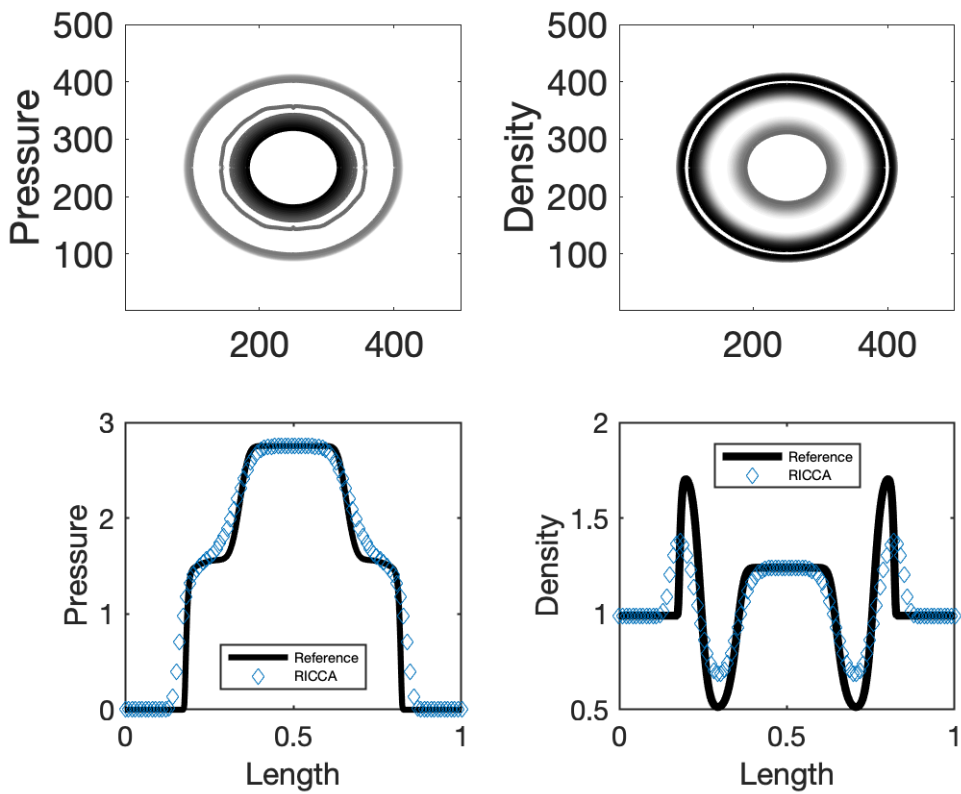


FIGURE 25 2D Line and contour plots of density and pressure using RICCA

4 Conclusions

Numerical simulations of Euler equations in 1D and 2D have been carried out using MOVERS (both scalar dissipation and vector dissipation), MOVERS+ and RICCA, for multicomponent gases with perfect gas EOS and stiffened gas EOS using mass fraction approach and γ -based approach in conservative form. It can be concluded that

1. both the numerical schemes RICCA and MOVERS+ can be extended to multicomponent gases with different EOS without any modifications,
2. both the numerical schemes preserve the mass fraction positivity and the pressure positivity in the conservative approach when used in mass fraction based model.
3. pressure oscillations are observed in the finite volume framework for interface only problem and when γ -based model is adopted no pressure oscillations are observed.
4. both these schemes can be easily extended to any number of components.
5. both the schemes can handle large jumps in γ without any modifications.

References

1. R. Abgrall, *An extension of Roe's upwind scheme to algebraic equilibrium real gas models*, Computers & Fluids **19(2)** (1991), p.p. 171-182.
2. R. Abgrall, *How to prevent pressure oscillations in multicomponent flow calculations: A quasi conservative approach*, J. Comput. Phys. **125** (1996), p.p. 150-160.
3. R. Abgrall, *Generalisation of the Roe scheme for the computation of mixture of perfect gases*, Rech. Aerosp., **6** (1988), pp. 31-43 (English edition).
4. R. Abgrall, S. Karni, *Computations of Compressible Multifluids*, Journal of Computational Physics **169** (2001), p.p. 594-623.
5. R. Abgrall, *Preliminary results on an extension of Roe approximate Riemann solver to non equilibrium flows*, [Research Report] RR-0987 (1989), pp.39. <inria-00075572>
6. J. Blazek, *Computational Fluid Dynamics Principles and Applications*, Elsevier Publications (2005).
7. D. Chargy, R. Abgrall, L. Fezoui, B. Larroutou, *Conservative numerical schemes for multicomponent inviscid flows*, Rech. Aerosp., **2** (1992), pp. 61-79 (English version).
8. P. Colella, H. Glaz, *Efficient Solution Algorithms for the Riemann Problem for Real gases*, Journal of Computational Physics **59** (1983), p.p. 264-289.
9. R.M.L. Coelho, P.L.C. Lage and A. Silva Telles, *A Comparison of hyperbolic Solvers for Ideal and Real gas flows*, Brazilian Journal of Chemical Engineering, **23**, p.p. 301-318.
10. T.J. Chung, *Computational Fluid Dynamics*, Cambridge University Press (2010).
11. G. Fernandez, B. Larroutou, *Hyperbolic schemes for multicomponent EULER equations*, in *Nonlinear Hyperbolic Equations Theory, Computation Methods, and Applications*, Vol. 24 of the series Notes on Numerical Fluid Mechanics, p.p. 128-138.
12. S. Jaisankar, S.V. Raghurama Rao, *A central Rankine-Hugoniot solver for hyperbolic conservation laws*, Journal of Computational Physics, **228(3)**(2009), p.p. 770-798.
13. S.Jaisankar and S.V. Raghurama Rao, *Diffusion regulation for Euler solvers*, Journal of Computational Physics, **vol. 221** (2007), pp. 577-599.
14. S. Karni, *Multicomponent flow calculations by a consistent primitive algorithm*, Journal of Computational Physics., **112** (1994), pp. 31-43.
15. S. Karni, S. Canic, *Computations of Slowly Moving Shocks*, Journal of Computational Physics **136** (1997), p.p. 132-139.
16. A. Kurganov and E. Tadmor, *New high-resolution central schemes for nonlinear conservation laws and convection-diffusion equations*, Journal of Computational Physics **160(1)** (2000), p.p. 241-282.
17. B. Larroutou, L. Fezoui, *On the equations of multicomponent perfect and real gas inviscid flow*, in *Non-Linear Hyperbolic Problems*, edited by Carasso, Charrier, and Joly, Lecture Notes in Mathematics, **1402**, (Springer Verlag, Heidelberg, 1989) p.p. 69.
18. B. Larroutou, *How to preserve the mass fractions positivity when computing compressible multi-component flows*, [Research Report] RR-1080 (1989). <inria-00075479>
19. M.S. Liou, *Mass flux schemes and connection to shock instability*, Journal of Computational Physics **160(2)**(2000), p.p. 623-648.
20. Liou, M.-S., and Steffen, C., *A New Flux Splitting Scheme*, Journal of Computational. Physics **107**(1993), p.p 23-39.

21. Liou, M.-S., *A Sequel to AUSM: AUSM+* Journal of Computational Physics, **129**(1996), p.p. 364-382.
22. Liou, M.-S., *A Sequel to AUSM, Part II: AUSM+-up*, Journal of Computational Physics, **214**(2006), p.p. 137- 170.
23. P.D. Lax, *weak solutions of nonlinear Hyperbolic Equations and their Numerical Computations*, Comm. Pure. Appl. Math. **VII** (1954), p.p. 159-193.
24. R.S. Lagumbay, *Modeling and Simulation of Multiphase/Multicomponent Flows*, Ph.D Thesis, University of Colorado, 2006.
25. Maruthi N.H., *Hybrid Central Solvers for Hyperbolic Conservation Laws*, PhD Thesis, Indian Institute of Science, Bangalore, India, 2016.
26. R. Menikoff, B.J. Plohr, *The Riemann problem for fluid flow of real materials*, Reviews of modern physics **61**(1)(1989), p.p. 75.
27. Ramesh Kolluru *Novel, Robust and Accurate Central solvers for Real, Dense and Multicomponent gases*, PhD Thesis, Indian Institute of Science, Bangalore, India, 2019.
28. P.L. Roe, Journal of Computational Physics **43** (1981), p.p. 357.
29. P.L. Roe, *Characteristic-based schemes for the Euler equations*, Annural Review of Fluid Mechanics, **vol. 18** (1986), pp. 337-365.
30. P.L. Roe, *Shock Capturing, Chapter 6, Handbook of Shock Waves*, , Academic Press, **vol. I** (2001), pp. 787-877
31. S.V. Raghurama Rao, S. Deshpande, Computational Fluid Dynamics Journal of Japan Society of CFD **4** (1995), p.p. 415.
32. V.V. Rusanov, *Calculation of interaction of non steady shock waves with obstacles*, NRC, Division of Mechanical Engineering (1962).
33. K.M. Shyue, *An Efficient Shock-Capturing Algorithm for Compressible Multicomponent Problems*, Journal of Computational Physics **142** (1998), p.p. 208–242.
34. K.M. Shyue, *A Fluid-Mixture Type Algorithm for Compressible Multicomponent Flow with van der Waals Equation of State*, Journal of Computational Physics **156** (1999), p.p. 43–88.
35. K.M. Shyue, *A Fluid-Mixture Type Algorithm for Compressible Multicomponent Flow with Mie Gruneisen Equation of State*, Journal of Computational Physics **171** (2001), p.p. 678–707.
36. K.M. Shyue, *A fluid-mixture type algorithm for barotropic two fluid flow problems*, Journal of Computational Physics **200** (2004), p.p. 718–748.
37. R. Saurel, R. Abgrall, *A simple method for compressible multifluid flows*, SIAM Journal on Scientific Computing **21**(3) (1999), p.p. 1115-1145.
38. R. Saurel, M. Larini and J.C. Loraud, *Exact and Approximate Riemann Solvers for Real Gases*, J. Comput. Phys., **112** (1994), pp. 126-137.
39. B. van Leer, *Flux-vector splitting for the Euler Equations*, in 8th International Conference on Numerical Methods in Fluid Dynamics, Springer (1982), p.p. 507-512.
40. B. van Leer, *Upwind and high-resolution methods for compressible flow: From donor-cell to residual distribution schemes*, Communications in Computational Physics, **vol. 1, no. 2** (2006), pp. 192-206.
41. N. Venkata Raghavendra, *Discrete Velocity Boltzmann Schemes for Inviscid Compressible Flows*, PhD Thesis, Indian Institute of Science, Bangalore, India, 2017.
42. N. Venkata Raghavendra, S. V. Raghurama Rao, *A Boltzmann scheme with physically relevant discrete velocities for Euler equations*. arXiv:1612.07911v1 [physics.comp-ph] 23 Dec 2016.

How to cite this article: Ramesh Kolluru., S V Raghurama Rao, and G N Sekhar, (2019), Simple, Accurate and Robust Algorithms for Multi-Component mixture equations with Stiffened gas EOS, , .